Thermal decomposition of divanadium pentoxide V_2O_5: Towards a nanocrystalline V_2O_3 phase

D.S. Su * and R. Schlögl

Department of Inorganic Chemistry, Fritz Haber Institute of the Max Planck Society, Faradayweg 4-6, D-14195 Berlin, Germany

Received 5 March 2002; accepted 4 July 2002

Thermal decomposition of V_2O_5 was studied by means of transmission electron microscopy (TEM) and electron energy-loss spectroscopy (EELS). Samples were heated in a specimen chamber of an electron microscope up to 600 °C in vacuum at 10^{-7} Torr. TEM and EELS reveal a sequence of transformations from V_2O_5 via VO_2 to V_2O_3, which differs from the electron-beam-induced reduction of V_2O_5. The phase transformation does not proceed topotactically. Our observation reveals that the initial thermal decomposition of V_2O_5 to V_2O_3 is followed by a combination of diffusion, coalescence, and stabilization processes. Our experiments open a new way for the preparation of single-crystalline V_2O_3 nano-particles.

KEY WORDS: V_2O_5; V_2O_3; thermal decomposition; reduction; TEM; EELS.

1. Introduction

The reduction behaviors and phase transitions of vanadium oxides at various temperatures have been well studied previously [1–7]. This is due to the fact that reduction and phase transition are phenomena accompanied in almost all catalytic processes using vanadium oxide-based catalysts. A great deal of work has been carried out to study the surface reduction of V_2O_5. For instance, a V_2O_5–V_6O_{13} transformation is reported at the V_2O_5 (001) surface by heating V_2O_5 (500 °C) in an O_2 atmosphere (5×10^{-4} Torr, 1 h) [1]. A cleaved V_2O_5 (001) surface can also be reduced to the V_6O_{13} (001) surface by a long-term exposure to an electron beam in a LEED chamber [2]. The mechanism for the transformation of V_2O_5 into V_6O_{13} occurring during the reduction is considered to be through ordering of oxygen vacancies: if every third oxygen layer in the V_2O_5 structure is removed, shearing occurs from corner-linked to edge-linked octahedra [3].

The earlier investigations on the bulk reduction of V_2O_5 were concentrated on the V_2O_5–H_2 reactions for the syntheses of vanadium oxides with oxidation states lower than 5+ [8–10]. Other methods for the reduction of vanadium oxide were also reported [11]. Gai studied defect nucleation and the growth of defect phases in reduced V_2O_5 using a gas-reaction cell in a high-voltage electron microscope; she found that the observed defects are a consequence rather than the origin of the catalytic activity [12]. Recently, V_2O_5–H_2 reductions were re-studied by *in situ* X-ray diffraction with respect to reduction kinetics and the geometry of phase transitions at various temperatures [13]. Thermal decomposition of a mixture of V_2O_3 and V_2O_5 was studied by Gillis by heating the sample at 600 °C in vacuum for eight days [5]. Phase transformations resulting in the co-existence of V_2O_5, V_6O_{13}, VO_2 and V_3O_7 were found. The thermal decomposition of bulk V_2O_5 at a temperature up to 400 °C in vacuum was investigated by Tilley and Hyde using TEM [4]. A number of new phases were reported, two of them being described as ordered super-lattices of anion vacancies in V_2O_5. These authors could not find any evidence for the occurrence of crystallographic shear, which is said to be necessary for the phase transformation.

Electron beam-induced reduction of V_2O_5 differs from the V_2O_5–H_2 reduction and from the thermal decomposition reported by Tilley *et al.* [4] and by Gillis [5]. High-resolution imaging [6], as well as electron diffraction and electron energy-loss spectroscopy (EELS) [7], reveal the V_2O_5–VO (in rock salt structure) transformation induced by high-voltage electron beam irradiation in the TEM. However, different pathways for this transformation were observed: while Fan *et al.* reported that V_2O_5 is firstly reduced to V_6O_{13} before VO is formed [6], Su *et al.* found that V_2O_5 is reduced to VO via an unknown intermediate phase (with the average oxidation state of vanadium near 3+) [7]. More recently, it was reported that if the electron beam-induced reduction is performed at liquid helium temperature, V_2O_5 can only be reduced to an amorphous phase with an average oxidation state of 4+ [14].

In the present work, we investigate the thermal decomposition of V_2O_5 on a heating stage of TEM, allowing the simultaneous electron diffraction, high-resolution imaging and electron energy-loss spectroscopic characterization of the transformation. The reasons for this work are as follows: first, we want to find out the reduction path of V_2O_5 under a controlled temperature condition and

* To whom correspondence should be addressed.

1011-372X/02/1100-0115/0

compare it with the reduction induced by electron-beam irradiation, both under the same vacuum condition. Second, the obtained knowledge about the reduction in a non-chemical ambient (high vacuum) can help us in understanding the phase transition in a more complicated chemical process. Third, the obtained results can serve as pre-knowledge for the preparation of vanadium oxide nanostructures, useful as model systems for catalytic selective oxidation reactions.

2. Experimental

A GATAN heating stage was used for the thermal decomposition of V_2O_5. The high vacuum of the specimen chamber was kept at 10^{-7} Torr. The sample was heated to 200, 400, 500, and 600 °C with a heating rate of 20 °C/min and kept for 1 h at each temperature. V_2O_5 crystals, prepared by chemical vapor transport reaction [15], were crushed gently in carbon tetrachloride. Due to the weakly bonded layer-structure [3], most of the crushed pieces were cleaved along the (001) plane. A drop of the solution containing the thin flakes was placed onto a copper mesh grid, covered with a holey carbon film and allowed to dry. A Philips CM200 FEG electron microscope, operated at 200 kV and equipped with a GIF100 GATAN imaging filter, was used. The imaging filter, operated in the spectroscopy mode, was used to record EEL-spectra. In order to obtain the near-edge structures of vanadium and oxygen atoms, all the measured EEL-spectra were corrected for background and multiple scattering [16].

3. Results

Figure 1 shows the vanadium L and oxygen K edges, extracted from EEL-spectra and recorded from V_2O_5, unheated and heated at 200, 400, 500 and 600 °C. The initial spectrum (RT) is typical for V_2O_5 in orthorhombic structure, characterized by the vanadium $2p \rightarrow 3d$ transitions (V L-edge) at 519 and 526.7 eV and oxygen $1s \rightarrow 2p$ transitions (O K-edge) above 530 eV. Heating the V_2O_5 sample caused two remarkable changes in the spectra: the vanadium L edge shifted to lower energy and the integral intensity of oxygen K edges decreased, indicating a preferred release of oxygen besides possible V_xO_y evaporation during the thermal decomposition. The peak energy of the L_3 edge of vanadium shifted to 518.3 eV at 400 °C, which is close to the peak position of VO_2 at 518.5 eV. The maximum of this peak shifted to even lower energy loss with increasing temperature and reached 517.4 eV at 600 °C, corresponding to the position of the L_3 edge maximum of V_2O_3. The phase formed at 600 °C is stable upon cooling down to room temperature. Figure 1 also shows the vanadium L and oxygen K edges of the sample after cooling down to room temperature. For comparison a reference spectrum of V_2O_3 is included in figure 1. The agreement of all three spectra is obvious.

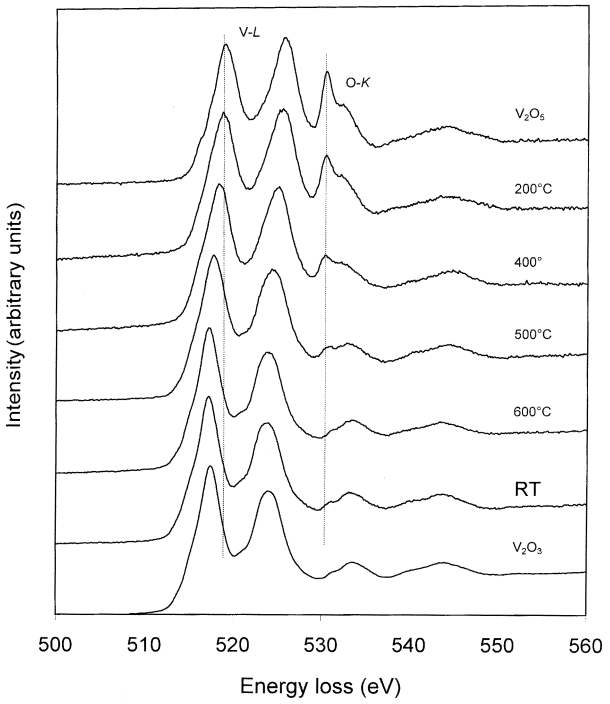

Figure 1. Vanadium L and oxygen K edges taken at various temperatures and after cooling down to room temperature (RT). For comparison, a reference spectrum from V_2O_3 is included. The spectra are corrected for background and multiple scattering.

An electron diffraction pattern taken at 500 °C from a thin sample flake is shown in figure 2(A). Before the heating, the diffraction pattern contained regularly arranged spots of single-crystalline V_2O_5. The pattern in figure 2(A) stems from randomly oriented crystallites formed through the thermal decomposition. This indicates that the phase transition did not occur topotactically. Figure 2(B) shows the rotationally integrated profile of this pattern. The profile contains both sets of peaks from VO_2 and V_2O_3: the diffraction peaks marked with lines can be identified as the ones of V_2O_3 in corundum structure, while the peaks marked with arrows indicate VO_2 in rutile structure. No peaks due to V_2O_5 were detected. This mixed phase can be quantitatively analyzed by matching the measured EEL-spectrum with the composed spectrum using the known VO_2 and V_2O_3 samples, as revealed in figure 4. The best matching is obtained by a spectrum with components of 36% from VO_2 and 64% from V_2O_3. Further heating of the sample to 600 °C produced a diffraction pattern from very thin crystallites of V_2O_3, in combination with a pattern from large crystallites containing intensities from VO_2. With prolonged heating of the sample at 600 °C for several hours, no reduction of V_2O_3 to other phases was observed. Therefore, we conclude that under the given conditions, V_2O_5 undergoes a phase transformation *via* VO_2 into V_2O_3.

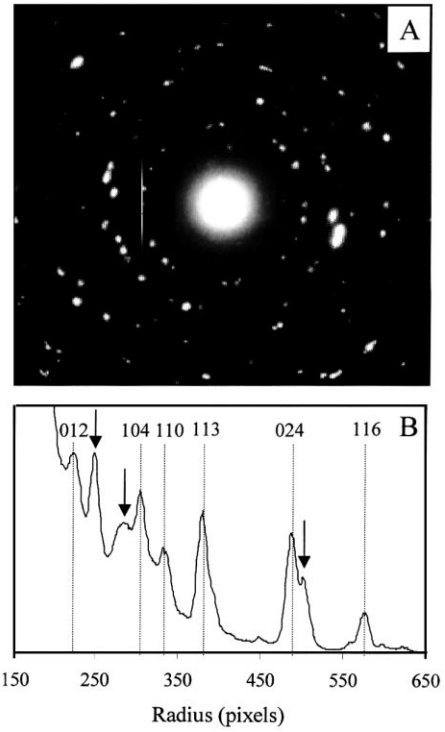

Figure 2. Electron diffraction pattern (A) taken at 500 °C and its rotationally integrated profile (B). Lined peaks are identified as from V_2O_3 (indexed) and arrowed peaks are from VO_2.

The electron micrograph in figure 4 taken at 500 °C shows how the morphology of the sample changes during the thermal decomposition. The decomposition proceeds faster for the initially thin V_2O_5 particle (on the left side of the micrograph) than for the thick particle (at the right side of the micrograph). This micrograph reveals details of the decomposition steps: the nucleation and growth of the V_2O_3 phase, determined by the atomic diffusion, and the formation of lattice defects during the phase transformation along microstructural defects of the parent V_2O_5. The intermediate defective state of the oxide is highly strained, as seen from the contrast in the electron micrograph (mainly on the left side). Since the diffusion occurs isotropically, at first the transformed phase forms spherical particles. Coalescence of the primary particles leads to worm-shaped objects. Spherical or worm-shaped particles exhibit a defect-rich surface and contain a high surface energy; stabilization through reduction of surface defects and minimization of the surface energy by a change of morphology should occur.

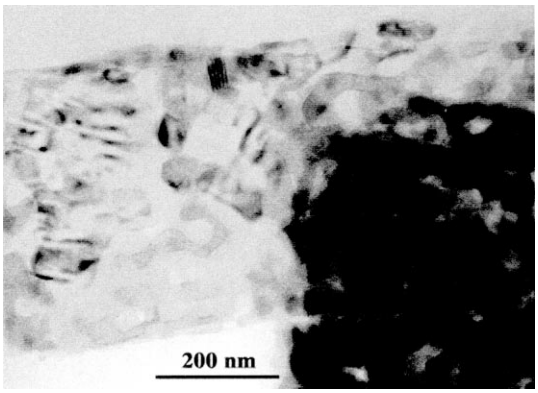

Figure 4. Low magnification electron micrograph taken at 500 °C showing the change of the morphology during the thermal decomposition.

The electron micrograph in figure 5, taken after heating at 600 °C, reveals the final stage of the phase

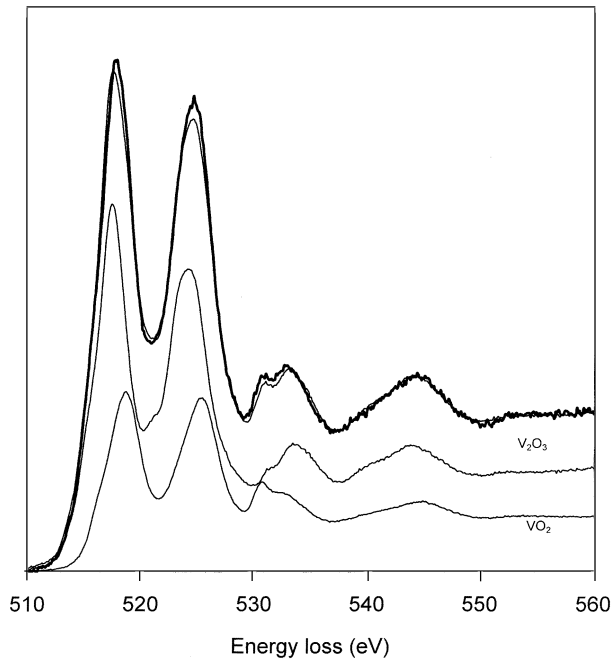

Figure 3. Matching of the measured EEL-spectrum at 500 °C (bold line) with a composed spectrum with 36% VO_2 component and 64% V_2O_3 component.

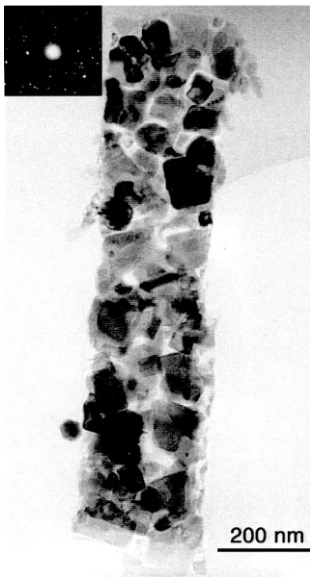

Figure 5. Electron micrograph of a V_2O_5 flake after heating at 600 °C, showing the formation of V_2O_3 nano-particles; the corresponding diffraction pattern is inserted.

transformation. Large V_2O_3 particles were observed. Although they exhibit a non-uniform morphology, most of them are shaped as regular hexagonal or square objects. High-resolution TEM shows that all these particles are single crystalline with well-ordered bulk and surface structures. Electron diffraction (inset) reveals again that all the formed V_2O_3 nano-particles are randomly oriented.

4. Discussion

We observed a thermal reduction of V_2O_5–VO_2–V_2O_3, which differs from the electron-beam-induced reduction under the same vacuum condition, by which V_2O_5 was found to be reduced to VO in rock-salt structure [7]. Thus, our results suggest that electron-beam damage cannot simply conject to a bulk temperature equivalent, and the effects of electron bombardment are complex and may operate quite differently from thermal decomposition of a bulk sample in vacuum.

Although we cannot observe a V_2O_5–V_6O_{13} transformation directly, such a transformation of it is not likely to be excluded if it, as mentioned above, occurs only at the surface. Our method is bulk sensitive. Another reason could be that the *lifetime* of V_6O_{13} is too short and it can be rapidly reduced. Our experiment on the thermal decomposition of V_2O_5 in a vacuum of 10^{-4} Torr in a sealed glass tube shows that heating overnight at 400 and 550 °C respectively does not induce significant changes of V_2O_5. One reason for this different observation could be the high vacuum we have in the specimen chamber (at least 10^{-7} Torr), in which the oxygen partial pressure is quite low. Furthermore, our experiment is performed under a dynamic vacuum condition (the chamber is pumped all the time). V_6O_{13} was obtained by reducing a mixture of V_2O_5 and V_2O_3 in a sealed platinum tube placed in an autoclave, but for a prolonged time (three days) and at an elevated temperature (650 °C) [11]. Reducing with CO and C_2H_4, the V_2O_5–V_6O_{13} transformation through crystallographic shearing was also reported [12]. However, the experimental conditions differ from ours, which might explain why the further reduction of vanadium and the formation of V_2O_3 nano-particles are observed in the present work.

Our observation suggests that no equilibrium in the system of V_2O_5, V_6O_{13}, and VO_2 can be achieved under the given vacuum condition at high temperature, while an equilibrium in the system of V_2O_3 is established. The obtained V_2O_3 particles are stable and no further reduction could be observed. Considering that the preparation of vanadium oxide clusters as model catalysts is performed in ultra-high vacuum condition, our result may suggest that a direct evaporation of V_2O_5 cannot result in the growth of vanadium clusters with an oxidation state higher than 4, simply due to the fact that V_2O_5 reduces already at temperatures lower than the melting point.

Our observation reveals that the thermal decomposition of V_2O_5 to V_2O_3 is followed by a combination of diffusion, coalescence, and stabilization processes, accompanied by the loss of oxygen from the very beginning. Since the diffusion occurs isotropically, the phase transformation does not proceed topotactically. The reduced phases are in spherical form and coalesce, giving the worm-shaped contrast in the electron micrograph (figure 3). The formation of V_2O_3 nano-particles in regular hexagonal or square form is a consequence of the surface energy minimization of the coalesced particles. However, this is only possible due to the absence of gas-phase oxygen or reductant gas (H_2 or CO); otherwise the process could proceed quickly.

The mechanism of V_2O_5–V_6O_{13} reduction is explained as an ordering of oxygen vacancies in V_2O_5: if every third oxygen layer in the [010] direction is removed, shearing in the [100] direction can lead to the formation of V_6O_{13} [3]. Recently, it was pointed out that by further removing oxygen atoms in every third oxygen layer and subsequently shearing in the same direction, VO_2 can be formed from V_6O_{13} by chemical reduction with hydrogen [10]. Lattices formed by such crystallographic shearing maintain the defined orientation relationship to the initial lattice. The resulting crystallite therefore should have a certain topotactical relationship to the initial crystals. The nano-particles shown in figure 5 are randomly oriented with respect to the initial V_2O_5 single crystal. Our results suggest that in the absence of a chemical reductant such a crystallographic shear mechanism cannot be applied to the V_2O_5–V_2O_3 or VO_2–V_2O_3 transformations. Further works on the reduction mechanism are needed.

5. Summary

We present in this preliminary report the thermal decomposition of V_2O_5 in high vacuum heated up to 600 °C. TEM and EELS reveal a sequence of transformations from V_2O_5 *via* VO_2 to V_2O_3. The thermal decomposition starts with the loss of oxygen. In the absence of gas-phase oxygen or reductant gas such as H_2 or CO, the decomposition occurs slowly, allowing the coalescence and the stabilization of the reduced phase. This leads to the formation of V_2O_3 nano-particles in regular shapes, with minimized surface energy and perfect bulk and surface structure. The rate of the reduction is related to the thickness of the crystal. The obtained results indicate that the thermal decomposition of V_2O_5 occurs in a different way than the electron beam-induced reduction of V_2O_5 under the same vacuum condition. Our findings open a new way for the preparation of single-crystalline V_2O_3 nano-particles.

Acknowledgement

The work is supported by the Deutsche Forschungsgemeinschaft SFB 546. D.S.S. thanks Dr. V. Roddatis for the prepartion of figure 3.

Reference

[1] K. Devriendt, H. Poelman and L. Fiermans, Surf. Sci. 433–435 (1999) 734.
[2] L. Fiermans and J. Vennik, Surf. Sci. 9 (1968) 187.
[3] J. Haber, M. Witko, and R. Tokarz, Applied Catalysis A-General 157 (1997) 3.
[4] R.J.D. Tilley and B.G. Hyde, J. Phys. Chem. Solids 31 (1970) 1613.
[5] E. Gillis, Compte Rend. Acad. Sci. Paris 258 (1964) 4765.
[6] H.J. Fan and L.D. Mark, Ultramicroscopy 31 (1989) 357.
[7] D.S. Su, M. Wieske, E. Beckmann, A. Blume, G. Mestl and R. Schlögl, Catal. Lett. 75 (2001) 81.
[8] Winfried Brückner, in: *Vanadiumoxide*, (Akademie Verlag, 1983).
[9] W. Klemm and P. Pirschner, Optik 3 (1948) 75.
[10] B. Belbeoch, R. Kleinberger and M. Roulliay, J. Phys. Chem. Sol. 39 (1978) 1007.
[11] K.-A. Wilhelmi, J. Waltersson and L. Kihlborg, Acta Chem. Scand. 25 (1971) 2675.
[12] P.L. Gai, Phil. Mag. A 48, No. 3 (1983) 359.
[13] H. Katzke *et al.*, to be published.
[14] M. Wieske, D.S. Su, E. Beckmann and R. Schlögl, Catal. Lett. in press.
[15] H. Schäfer, in: *Chemische Transportreaktionen* (Verlag Chemie, 1962).
[16] R. Egerton, *Electron Energy-Loss Spectroscopy in the Electron Microscope* (Plenum Press, New York, 1996).